MULTIWAVELENGTH STUDY OF S5 1803+784 DURING 2020 AND 2021 FLARES

Joseph Omojola[1,2], Andrew Chen[1], Justin Finke[3], Filippo D'Ammando[4]
On behalf of the *Fermi*-LAT Collaboration

[1]School of Physics, University of the Witwatersrand, Johannesburg, 2050, South Africa. email: 1926749@students.wits.ac.za
[2]Department of Physics, Federal University of Lafia, Lafia, 95001, Nigeria.
[3]US Naval Research Laboratory Code 7653, 4555 Overlook Ave SW, Washington, DC, 20375-5352, USA.
[4]Istituto Nazionale di Astrofisica (INAF), Istituto di Radioastronomia (IRA) via Piero Gobetti 101, 40129, Bologna, Italy.

Introduction

We report the spectral and temporal analysis of S5 1803+784 during the 2020 and 2021 flares. S5 1803+784 has Right Ascension (J2000) = $270.1891°$ and Declination (J2000) = $+78.4678°$ and redshift z = 0.684. Its characteristic weak optical emission lines and the spectral energy distributions (SEDs) high energy emission have often been modelled as a synchrotron self-Compton-only (SSC-only) BL Lac object. Here, we model the simultaneous broadband SED during the 12 April 2021 flare both as SSC-only and SSC+EC inverse Compton scattering. Where EC is the external inverse Compton component.

Motivation

This source is interesting for studying blazar jets due to its unprecedented recent bright flares [1] (Fig. 1).

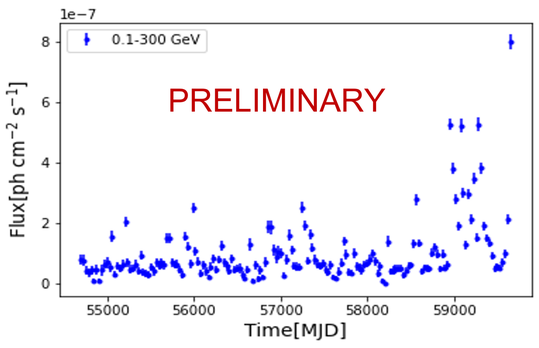

Fig. 1. 30-day binned γ-ray light curve from 2008-08-04 to 2022-03-30

Multiwavelength light curves

Fermi-LAT observed S5 1803+784 in a flaring state in April 2020, with maximum γ-ray flux detected around April 12, 2020 (MJD 58951). The data were analyzed following the standard procedures implemented in the *Fermi* ScienceTools (ver. 1.2.23) using Fermipy (0.20.0) analysis thread [2]. The simultaneous data within this period were obtained from various instruments at different energy bands (Fig. 2): the optical flux from the Asteroid Terrestrial-impact Last Alert System (ATLAS) observatory, the X-ray fluxes in the energy range 0.3 - 10 keV from the *Swift*/XRT at and the 15 GHz radio fluxes from the Owens Valley Radio Observatory 40 m Telescope (OVRO) archive.

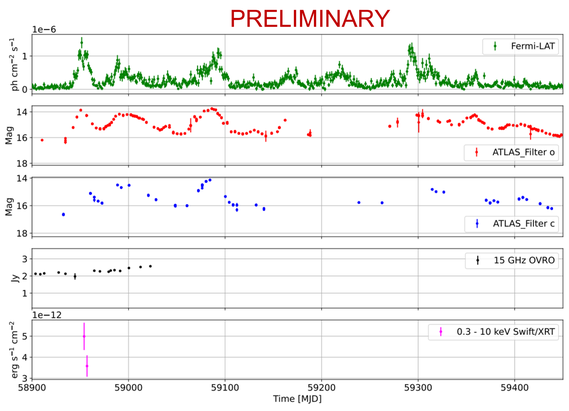

Fig. 2. Multiwavelength light curves

γ-ray flare profile

The flare temporal profile plots (middle panel of Fig. 3) using Eqn. 1 are based on the Bayesian blocks [3] in the upper panel of Fig.3.

$$F(t) = F_c + F_0\left(e^{\frac{t_0-t}{t_r}} + e^{\frac{t-t_0}{t_f}}\right)^{-1}, \quad (1)$$

where F_0 is the peak flux of the flare, F_c is the constant level of the quiescent flux, and t_0 is the time of the flux peak. Flare A, rise time, t_r, = 2.93 days, and the flare fall/decay time t_f = 1.82 days.
The γ-ray spectrum of Flare A produces the best fit with the log parabola (LP) distribution (Eqn. 2) and is compared with the power law (PL) distribution (lower panel of Fig. 3).

$$\frac{dN}{dE} = K\left(E/E_0\right)^{-(\alpha+\beta\log(E/E_0))} \quad (2)$$

where K is the normalization constant, α is the spectral index at energy E_0, and β is the spectral curvature.

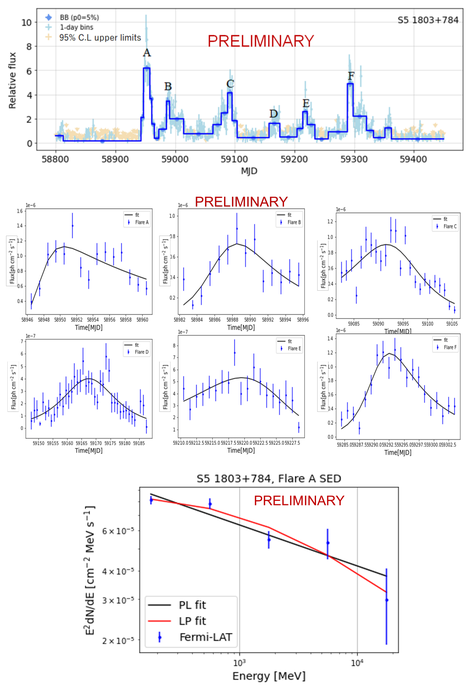

Fig. 3. (upper panel) Bayesian blocks [3], (middle panel) Flares fit to Eqn. 1., (lower panel) Flare A LP and PL spectra.

SED modelling

The spherical blob emitting region is filled with relativistic particles (electrons) with magnetic field strength B. The emitting particles move with a bulk Lorentz factor Γ along the jet, and Doppler beamed with a factor δ. The energy spectrum of the relativistic electrons is described by a broken power law. The size of the emitting region (R) is constrained with $R \leq c\delta t_{var}/(1+z)$ where t_{var}= t_f ln2 and the Doppler factor δ of 12.2 [4]. Using t_{var} the size of the emitting region is constrained to $R \leq$ 2.36 $\times$ 10^{16}cm. The distance of the emitting region from the black hole (R_H) is estimated using $R_H \approx 2c\Gamma^2 t_{var}/(1+z)$. The bulk Lorentz factor Γ is 9.45 [4] $\therefore$R$_H$ = 5.00 $\times$ 10^{17}cm. $L_{\rm Disk}$, the radius of the dusty torus(DT)(R_{DT}), $T_{\rm Disk}$, and T_{DT} are fixed during the spectral fit to the quiescent SED in Table 1.

Table 1: Quiescent state jet parameters

Symbol(Unit)	Jet parameters
$R_H(10^{17}\rm cm)$	5.00
$L_{\rm Disk}(10^{44}$ erg s$^{-1})$	2.12±0.12
$R_{DT}(10^{18}\rm cm)$	1.15±0.04
$T_{\rm Disk}(10^4\rm K)$	3.02±0.98
τ_{DT}	0.1
$T_{DT}(\rm K)$	655±107

SED modelling Cont.

The SED model and plots in Figs. 4 and 5 were achieved using JetSeT code [5][6][7].

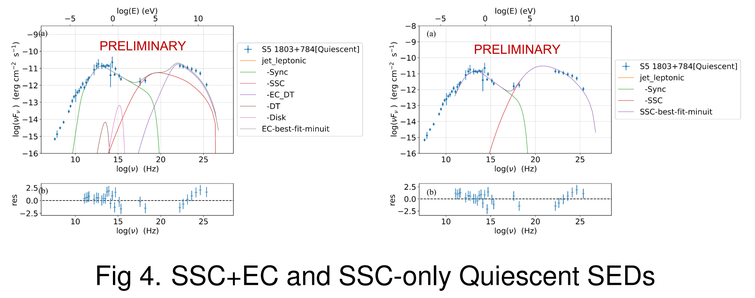

Fig 4. SSC+EC and SSC-only Quiescent SEDs

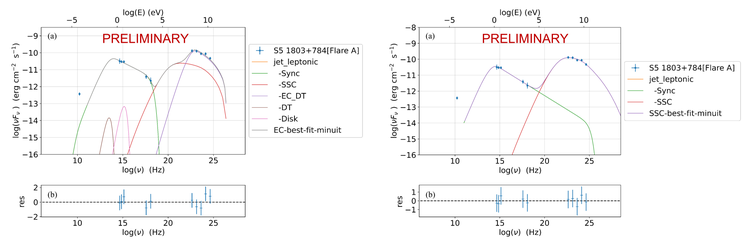

Fig 5. SSC+EC and SSC-only Flare A SEDs

Table 2: SED model fit parameters

Symbol(Unit)	Quiescent	Flare A (EC)	Flare A (SSC)
$\gamma_b \times 10^3$	$0.72^{+0.06}_{-0.05}$	$1.36^{+0.03}_{-0.03}$	$4.65^{+0.59}_{-0.38}$
p	$1.62^{+0.11}_{-0.12}$	$1.87^{+0.08}_{-0.08}$	$1.71^{+0.08}_{-0.09}$
p_1	$3.58^{+0.13}_{-0.11}$	$3.54^{+0.10}_{-0.09}$	$3.61^{+0.15}_{-0.11}$
$\gamma_{\rm min}$	$14.74^{+0.89}_{-0.82}$	$32.31^{+1.93}_{-3.78}$	$868^{+2.01}_{-4.00}$
$\gamma_{\rm max} \times 10^5$	$8.26^{+0.19}_{-0.13}$	$9.56^{+0.37}_{-1.20}$	$9306.56^{+1575.43}_{-1763.35}$
$R \times 10^{16}$ cm	$10.39^{+1.81}_{-1.64}$	$3.42^{+0.00}_{-0.00}$	$3.42^{+0.00}_{-0.00}$
δ	$12.20^{+0.00}_{-0.00}$	$26.07^{+2.41}_{-1.91}$	$25.70^{+2.41}_{-1.91}$
B (G)	$0.36^{+0.03}_{-0.03}$	$0.37^{+0.01}_{-0.01}$	$0.13^{+0.01}_{-0.01}$
N (cm^{-3})	$5.10^{+0.32}_{-0.29}$	$11.59^{+3.35}_{-2.64}$	$8.16^{+1.01}_{-1.03}$
χ^2/dof	29.69/18	4.21/2	1.56/2

Implications and conclusion

This is the first simultaneous broadband SED of the April 2020 flare that includes simultaneous X-ray emission and the X-ray being dominated by the synchrotron tail during the flare and not during the quiescent emission. The F-test and multiwavelength SED show that external photon from the DT is favourable for the γ-ray emission both during the flare and the quiescent states. The very high γ_{max} in the SSC-only flare SED is an unlikely model. The flare SED shows an interesting particle acceleration feature mentioned above whereby the X-ray emission undergoes a transition from being due primarily to the low-energy end of the inverse Compton emission in the quiescent state to coming primarily from the upper tail of the synchrotron emission. Both models show a hard low-energy spectral slope and a compact emitting region consistent with magnetic dissipation. The γ-ray emitting region constraint with the variability time-scale and the SED model parameters are consistent with the single-zone leptonic model.

Acknowledgements

The *Fermi*-LAT Collaboration acknowledges support for LAT development, operation and data analysis from NASA and DOE (United States), CEA/Irfu and IN2P3/CNRS (France), ASI and INFN (Italy), MEXT, KEK, and JAXA (Japan), and the K.A. Wallenberg Foundation, the Swedish Research Council and the National Space Board (Sweden). Science analysis support in the operations phase from INAF (Italy) and CNES (France) is also gratefully acknowledged. This work was performed in part under DOE Contract DE-AC02-76SF00515. ATLAS

- Prof. T Burnett (for the Bayesian blocks code)

References

[1] Venters, T., Angioni, R., and Ojha, R. 2020, 13633, 1. https://ui.adsabs.harvard.edu/abs/2020ATel13633.1V. [2] Wood, M., Caputo, R., Charles, E., et al. 2017, 301, 824. https://ui.adsabs.harvard.edu/abs/2017ICRC...35..824W. [3] Scargle, J. D., Norris, J. P., Jackson, B., et al. 2013, 764, 167, doi: 10.1088/0004-637X/764/2/167. [4] Hovatta, T., and Lindfors, E. 2019, 87, 101541, doi: 10.1016/j.newar.2020.101541. [5] Tramacere, A. 2020, ascl:2009.001. https://ui.adsabs.harvard.edu/abs/2020ascl.soft09001T. [6] Tramacere, A., Massaro, E., and Taylor, A. M. 2011, 739, 66, doi: 10.1088/0004-637X/739/2/66. [7] Massaro, E., Tramacere, A., Perri, et al. 2006, 448, 861, doi: 10.1051/0004-6361:20053644.